BNL-80249-2008-CP

Nonlinear Seismic Correlation Analysis of the JNES/NUPEC Large-Scale Piping System Tests

Jinsuo Nie, Giuliano DeGrassi, Charles H. Hofmayer, and Syed A. Ali*

Presented at the PVP 2008 Conference
Chicago, Illinois, USA
July 27-31, 2008

Energy Science and Technology
Nuclear Energy and Infrastructure Systems Division/NE

(* U.S. Nuclear Regulatory Commission)

Brookhaven National Laboratory
P.O. Box 5000
Upton, NY 11973-5000
www.bnl.gov

DISCLAIMER

Proceedings of PVP2008
2008 ASME Pressure Vessels and Piping Division Conference
July 27-31, 2008, Chicago, Illinois, USA

PVP2008- 61881

NONLINEAR SEISMIC CORRELATION ANALYSIS OF THE JNES/NUPEC LARGE-SCALE PIPING SYSTEM TESTS

Jinsuo Nie, Giuliano DeGrassi, Charles H. Hofmayer
Energy Science & Technology Department
Brookhaven National Laboratory
Upton, NY 11973-5000, USA
Email: jnie@bnl.gov

Syed A. Ali
Division of Engineering
Office of Nuclear Regulatory Research
U.S. Nuclear Regulatory Commission
Washington, DC 20555-0001

ABSTRACT

The Japan Nuclear Energy Safety Organization/Nuclear Power Engineering Corporation (JNES/NUPEC) large-scale piping test program has provided valuable new test data on high level seismic elasto-plastic behavior and failure modes for typical nuclear power plant piping systems. The component and piping system tests demonstrated the strain ratcheting behavior that is expected to occur when a pressurized pipe is subjected to cyclic seismic loading. Under a collaboration agreement between the U.S. and Japan on seismic issues, the U.S. Nuclear Regulatory Commission (NRC)/ Brookhaven National Laboratory (BNL) performed a correlation analysis of the large-scale piping system tests using detailed state-of-the-art nonlinear finite element models. Techniques are introduced to develop material models that can closely match the test data. The shaking table motions are examined. The analytical results are assessed in terms of the overall system responses and the strain ratcheting behavior at an elbow. The paper concludes with the insights about the accuracy of the analytical methods for use in performance assessments of highly nonlinear piping systems under large seismic motions.

DISCLAIMER NOTICE - The findings and opinions expressed in this paper are those of the authors, and do not necessarily reflect the views of the U.S. Nuclear Regulatory Commission or Brookhaven National Laboratory.

INTRODUCTION

JNES/NUPEC conducted a multi-year test program for the Ministry of Economy, Trade and Industry (METI) of Japan to investigate the behavior of typical nuclear power plant (NPP) piping systems under large seismic loads. The objectives of this program were to develop a better understanding of the elasto-plastic response and ultimate strength of nuclear piping systems, to ascertain the seismic safety margins in current piping design codes, and to assess new code allowable stress rules. The test program included monotonic and cyclic loading tests of piping material specimens, static and dynamic tests of piping components such as elbows and tees, seismic shaking table tests of two simple piping systems, and seismic shaking table tests of representative large-scale piping systems. The JNES/NUPEC large-scale piping system tests included two series of tests: design method confirmation tests and ultimate strength tests, with the former tests reported to attain a maximum stress level of 13.5 S_m and the latter tests to a maximum stress level of 24 S_m.

As part of collaborative efforts between the United States and Japan on seismic issues, NRC/BNL participated in this program by performing analyses for selected tests, and by evaluation of program results. The major objective of the NRC/BNL nonlinear finite element (FE) analyses was to investigate and evaluate the adequacy of state-of-the-art methods for predicting the elasto-plastic response of piping

systems subjected to large earthquake loads. The nonlinear FE analyses were performed using the ANSYS computer program, a code widely used in the nuclear industry. Nonlinear material models were developed based on the material and component test results. For the large-scale piping system tests, analysis of any test involved two phases: 1) a transient analysis of a whole piping system FE model (with plastic pipe elements and a multi-linear kinematic hardening material model) to obtain the displacement and acceleration responses for the entire piping system, and 2) a static analysis of an elbow model (with finite strain shell elements and the Chaboche nonlinear kinematic hardening material model) to obtain the strain responses. Analyses were performed for both the design method confirmation tests and the ultimate strength tests.

This paper presents a summary of the NRC/BNL nonlinear correlation analysis of the JNES/NUPEC large scale piping system tests and the insights gained from this study [1].

RELEVANT JNES/NUPEC TESTS

Material Tests

JNES/NUPEC carried out a series of static monotonic loading and cyclic loading tests to develop stress-strain curves and properties for typical piping materials. In the monotonic loading tests, the specimens were tensile tested to failure. A typical (engineering) stress-strain curve for STS410 carbon steel is shown by the dotted line in Figure 1, up to a strain of 5%. In the cyclic loading tests, the specimens were subjected to strain-controlled incremental cycling. These tests provided stress-strain hysteresis curves and also provided cyclic stress-strain curves for the materials for strains up to 2.5%.

Piping Component Tests

JNES/NUPEC also conducted static and dynamic tests on typical piping components which included elbows, tees, nozzles and reducers. In the cyclic loading tests, the test specimens were pressurized to induce an internal pressure stress equal to S_m, and then subjected to quasi-static sinusoidal displacements until a fatigue crack developed. The strain versus cycle plots illustrated the accumulation of ratcheting strain during the tests, as shown in Figure 3.

Large-Scale Piping System Tests

In the final phase of their test program, JNES/NUPEC performed a series of seismic shaking table tests on a representative large-scale piping system. The test specimens were Schedule 40 carbon steel (STS410) pipes with a nominal diameter of 200 mm (8 inch). Two series of tests were performed using the large high performance shaking table at the Tadotsu Engineering Laboratory. The first was a design method confirmation (DM) test and the second was an ultimate strength (US) test. The three-dimensional routing of the DM test specimen represented typical configuration characteristics of safety-related Japanese NPP piping systems. The piping system included straight pipe, nine elbows, a tee, and a 1000 kg (2200 lb) added mass representing a valve as illustrated in Figure 6. The system was supported by nozzles, an anchor, three two-directional supports, a horizontal support, a vertical support and a spring hanger. The US Test specimen had an identical piping configuration with the same piping components. Since this test was designed to stress the pipe to failure, it was modified by the addition of another 1000 kg (2200 lb) mass and the removal of a lateral support.

CHARACTERISTICS OF THE INPUT MOTIONS

A summary of the test cases is presented in Table 1 and Table 2. In all of these tests, the piping systems were internally pressurized to induce a hoop stress equal to the design stress intensity S_m. The tests were conducted at room temperature.

The input motions to the piping systems in the analysis were taken as the acceleration time histories recorded at the top of the shaking table. The time increment is 0.005 seconds for all acceleration time histories. Only the significant shaking table input motions were considered in this study. Furthermore, only selected tests are presented in this paper as space permits.

Motions from the DM Tests

The DM test included preliminary tests (DM1), allowable stress tests (DM2), and elasto-plastic response tests (DM4). Preliminary tests included sine sweep tests (DM1-1) to determine the natural frequencies and modal damping values, and unidirectional off-resonance seismic tests (DM1-2). For the DM2-1 test and the DM2-2 test, seismic table motions were applied simultaneously in the horizontal and vertical directions, and were selected to induce maximum stresses of $3S_m$ (primary stress limit) and $4.5S_m$, respectively. The DM4 series of elasto-plastic response tests applied higher input motions to achieve plasticity with stress levels from 2 to 4.5 times the primary stress limit, with the seismic waves adjusted so that the dominant input motion frequency was on-resonance. No evidence of pipe failure was observed. Figure 4 shows the acceleration time histories and their 5% response spectra for tests DM4-1 and DM4-2(2), respectively. For the DM4 tests, the dominant frequency is about 6 Hz, which is on resonance to the piping fundamental frequencies. The durations of the input motions for the DM4 tests are 82 seconds.

Motions from the US Tests

The US test was designed to fail the pipe. This test series included preliminary low-level sine sweep tests (US1) to determine the frequencies and modal damping values, and ultimate strength seismic tests (US2). The seismic input motion for US2 tests was designed to induce a maximum stress of $24S_m$, with the seismic waves adjusted so that the dominant input motion frequency was on-resonance. The seismic table motion was applied only in the horizontal direction. The seismic input motion was repeated until failure occurred. During the fifth test run, a longitudinal through-wall

crack developed in elbow 2 (see Figure 6), which was confirmed to be a result of fatigue ratcheting. The time history of the US2-1 test and its 5% damping response spectrum are shown in Figure 5. The dominant frequency can be determined to be about 3.6 Hz, which equals the fundamental frequency of the piping system measured for the US2-1 test, as shown in Table 2. The duration of the US2-1 input motion is 120 seconds.

All input motions, recorded at the top of the shaking table, were found to include large unrealistic drifting displacements. Therefore, all input motions were adjusted using a Lagrange-multiplier based correction algorithm [2]. Using the horizontal input motion of DM4-1 as an example, the original record appeared to reach a residual displacement of about 65 m in a monotonic fashion, which is unrealistic and will probably shadow the displacement response that is in a magnitude of millimeters. It was found that the change of the acceleration due to baseline correction was almost unnoticeable. The baseline correction changed only the low frequency content and the dominant frequency content was almost identically preserved by the baseline correction.

FINITE ELEMENT MODELING AND ANALYSES

The nonlinear analyses were performed using the ANSYS ver. 11 finite element (FE) code. Each of the nonlinear analyses for the large-scale pipe tests consists of two phases: (1) a transient analysis of the whole piping system using plastic pipe elements was performed to obtain the overall responses; (2) a static analysis of one of the elbows using plastic shell elements was carried out with displacement boundary conditions extracted from the piping system analysis to obtain the ratcheting strain responses. Accordingly, for the DM specimen and the US specimen, two FE models were developed to obtain the analytical responses. This modeling strategy is to facilitate an efficient computation for these tests. Automatic time stepping and occasionally the solution stabilization option were used.

Material Models

To represent the stress-strain relationship accurately for the strain range exhibited by the DM and the US tests, the multi-linear kinematic hardening model and the Chaboche nonlinear kinematic hardening model [4] were used in this study. Both hardening models are based on the Von Mises yield criterion and the associated flow rule. The multi-linear hardening rule does not permit the change of plastic modulus due to the presence of a mean stress, and consequently cannot predict strain ratcheting for a stress-controlled loading and unloading test. On the other hand, the Chaboche nonlinear hardening rule allows strain ratcheting because its plastic modulus contains a combination of several exponential functions of the plastic strain.

Multi-linear Kinematic Hardening Model This model was utilized in the transient analysis of the whole piping system (the 1st phase), which consisted of straight and curved plastic pipe elements. The ANSYS pipe elements do no accept the more advanced Chaboche nonlinear kinematic hardening rule. As required in large strain analysis, the true stress-strain curve was used to obtain the parameters for this model. As shown in Figure 1, four straight segments were fitted over four strain ranges on the true stress-strain curve, for a strain range below 5%. The segment designed Sig_e represents the elastic domain, and the Sig_1 to Sig_3 segments represent the multi-linear plastic domains. The ANSYS multi-linear model was then created by identifying the Young's modulus and the intersection points between the nearby line segments from Figure 1. The Young's Modulus was found to be 1.8866e5 MPa, and the corner points are (0.146 %, 275.942 MPa), (2.184 %, 280.140 MPa), (2.701 %, 312.550 MPa), and (5.000 %, 379.340 MPa).

Chaboche Nonlinear Kinematic Hardening Model This model was used in the static analysis of the elbow model (the 2nd phase), which was modeled with nonlinear shell elements to capture the strain ratcheting effect in the tests. The Chaboche hardening rule is a superposition of several "decomposed" Armstrong-Frederick hardening rules [3]. A three-decomposed-rule model as commonly adopted in the literature [3, 5] was used in this study. The three rules, designated by the backstresses as α_1, α_2, α_3, simulate three portions of a plastic stress-strain curve respectively, namely the initial high plastic modulus at the onset of yielding, the transient nonlinear portion of the plastic stress-strain curve, and the linear part of this curve for high strain values [4, 5]. The third rule (α_3) is a linear rule and, with a key parameter $\gamma_3 = 0$, can result in a complete shakedown. Therefore, a small positive γ_3 was recommended by Chaboche [4] to improve the ratcheting capability of the 3-rule model while imposing no significant change to the hysteresis loop. More recently, Bari and Hassan [5] suggested that instead of using a monotonic stress-strain curve, a uniaxial strain-controlled stable hysteresis curve should be used to develop the parameters for the 3 rules (excluding γ_3). The parameter γ_3 can be determined later by fitting a uniaxial ratcheting experiment. This approach was utilized by DeGrassi and Hofmayer [3] with exception for γ_3, which was however determined from the results of a strain-controlled cyclic test of an elbow component by JNES/NUPEC.

It was observed in the literature that the simulated forward loading curve by the so-developed Chaboche nonlinear kinematic material models did not agree particularly well to the test at the transient region [see 3, 5 for example]. In this study, a more rigorous approach was taken in developing the parameters for the Chaboche model (except for γ_3). For the convenience of discussion, the equations for the Chaboche model are summarized as,

$$\sigma_x = \sigma_y + \alpha_1 + \alpha_2 + \alpha_3 , \qquad (1)$$

$$\alpha_i = \frac{C_i}{\gamma_i}\left[1 - 2\exp\left\{-\gamma_i\left(\varepsilon_p - \varepsilon_{p|}\right)\right\}\right], \text{ for } i = 1 \text{ or } 2 , \qquad (2)$$

$$\alpha_3 = C_3 \varepsilon_p \,, \qquad (3)$$

where σ_x is the total axial stress, σ_y the yield stress, ε_p the plastic axial strain, ε_{pl} the plastic strain limit of the stable hysteresis loop, C_i and γ_i the parameters for the three "decomposed" Armstrong-Frederick hardening rules α_i (backstresses). The elastic modulus and the yield stress were identified previously in developing the multi-linear hardening model.

Using the JNES/NUPEC strain-controlled uniaxial cyclic test data of an STS410 steel specimen, DeGrassi and Hofmayer developed a forward loading curve to derive the parameters (except for γ_3) for the Chaboche model [3]. The same forward loading curve was used in this study, in the form of a true stress-strain curve with the elastic strain removed. A least-square minimization of the difference between the test curve and the developed curve (from Eq. 1) can yield an optimal set of parameters. The initial values of C_1 and C_3 were determined by fitting the elastic portion and the very end of the linear portion of the test forward loading curve. The initial values of C_2, γ_1, and γ_2 were taken from reference [3]. Only C_1, C_2, γ_1, and γ_2 participated in the least-square minimization; while C_3 kept the initial value in order to maintain the linear portion of the plastic stress-strain curve. As shown in Figure 2, an excellent match can be seen between the test curve and the Chaboche model σ_x developed with the above optimal parameters. It can also be observed in Figure 2 that the optimal parameters do not change the original intention of the three rules as proposed by Chaboche [4]. Explicitly speaking, the three rules of the optimal Chaboche model still represents the initial high plastic modulus portion, the transient nonlinear portion, and the linear portion of the plastic stress-strain curve, respectively.

Using the same approach as by DeGrassi and Hofmayer [3], the parameter γ_3 was determined by performing a parametric study of γ_3 using the strain-controlled cyclic test of an elbow component. By varying γ_3, while maintaining other parameters, a series of trial-and-error analyses were carried out using an ANSYS shell model, and a value of γ_3 was then found to achieve the best prediction of the strain ratcheting behavior of the elbow component. Figure 3 shows a comparison of the final hoop and axial strain ratcheting behaviors between the test and the analysis.

In summary, the Chaboche nonlinear kinematic hardening material model was established by the follow parameters: σ_y=275.92 MPa, E =203000 MPa, C_1 =65191.29 MPa, C_2 =14909.91 MPa, C_3 =1653.90 MPa, γ_1 =1044.83, γ_2 =177.06, and γ_3 =2.2.

Finite Element Models

Piping System Model for the DM tests Figure 6 shows the ANSYS FE model of the piping system. The straight pipe segments are discretized by mostly 500 mm long plastic straight pipe elements (PIPE20); while the elbows are represented by 4 plastic curved pipe elements (PIPE60). The average as-built diameter and the average as-built thickness of the piping specimen were used in the ANSYS model, with their values being 219.2 mm and 10.38 mm, respectively. The mass density of the pipe material was increased to 12,388 kg/m^3 to take into account the mass of the water. The added weight (1000 kg) in the test was represented by an ANSYS MASS21 element at node 35.

The internal pressure (10.7 MPa) and the gravity load were appropriately applied in the analyses. The spring hanger was represented by a concentrated force at node 35, which was determined as the static reaction force under gravity assuming a vertical support at this location. Restraints were modeled appropriately as shown in Figure 6. Some of these restraints and the fixed boundary conditions were replaced by the acceleration time history in the transient analyses. The fundamental frequencies using the multi-linear kinematic hardening model were calculated to be 5.88 Hz, slightly smaller than the measured values in the range of 5.9 to 6.3 Hz.

A Rayleigh damping model with only the stiffness term (BETAD) was used for the transient analyses. The damping value BETAD was determined using the fundamental frequency and measured damping ratio for the DM2-1 test as shown in Table 2.

Three responses taken at locations around Elbow 2 were selected for comparison with the tests, including:

- D2: the relative displacement between nodes 30 and 34.
- A2: the X directional absolute acceleration at node 29.
- S85: strains at a location on the exterior surface of elbow 2, which were designated in the test by strain gauge SE2C-7A (axial) and SE2C-7H (hoop). Strain responses are taken from the elbow shell model.

The relative displacements and rotations between node 30 and node 34 were also saved as inputs to the elbow shell models. The same set of outputs was also utilized for the analyses of the US tests.

Piping System Model for the US tests The overall configuration of the US tests is very similar to that of the DM tests as shown in Figure 6, except that the X direction restraint at node 13 was removed, another 1000 kg concentrated mass at node 29 and small masses at the constraint locations were added. The average as-built diameter and the thickness for this specimen were identified as 219.1 mm and 10.16 mm, respectively. Except for the shaking table motions, other loading and boundary conditions are the same as in the DM tests.

Using the first two modal frequencies 3.8 Hz and 6.4 Hz and the corresponding damping ratios 0.9% and 1.2%, the ALPHAD (mass term) and BETAD (stiffness term) of the Rayleigh damping model were determined to be 0.138 and 5.113e-4, respectively.

Using the multi-linear kinematic hardening model, the piping system model for the US tests predicted a fundamental frequency of 3.59 Hz, almost identical to the measured from the US2-1 test.

Elbow Model for the DM tests Elbow 2 between nodes 30 and 34 was further modeled using plastic shell elements to obtain the ratcheting strain responses. It has a centerline length of 950 mm for each branch and a radius of 304.8 mm for the elbow. The straight pipe segments are 645.2 mm long and are used to facilitate the simplification of boundary conditions at nodes 30 and 34. The diameter of the pipe is 219.2 mm (as-built) and its wall thickness is 10.38 mm (as-built).

As shown in Figure 7, Elbow 2 is modeled entirely with the ANSYS plastic SHELL181 elements for both the straight pipe branches and the elbow. The elbow model has a total of 1152 shell elements. The ANSYS shell element SHELL181 is a 4-node finite strain shell element that is suitable for large rotation and large strain nonlinear simulation of thin to moderately thick shell structures [6]. For nonlinear analysis, this element can take into account the change of shell thickness. In this study, a full integration scheme was used, which means that the strain response is not constant over an element. The Chaboche nonlinear kinematic hardening material model was used in the elbow shell model.

The boundary condition at each end of the elbow model was specified with a *rigid surface constraint* that couples the motion of the edge nodes to a single pilot node (30 or 34) at the centerline. While the pilot node 34 was restrained in all six degrees of freedom, the six differential displacement/ rotation time histories obtained from the piping system analysis were applied at the pilot node 30. The gravity and the internal pressure were applied in the elbow model. Since the analyses were static, damping and local inertial effects were not included.

The only responses obtained from this elbow shell model were the hoop and axial strain time histories in the vicinity of the strain gauges SE2C-7A (axial) and SE2C-7H (hoop), as indicated in Figure 7. This location is close to the top (+Z direction) on the exterior surface of the elbow at the symmetry plane. Four elements close to this location were chosen for use in the comparison to the test results.

Elbow Model for the US tests This elbow model is the same as that for the DM tests except for a different as-built pipe diameter and wall thickness, which are 219.1 mm and 10.16 mm, respectively.

RESULT ASSESSMENT

The DM Tests

The three elasto-plastic tests have significant accumulation of plasticity at elbows, which may change the dynamic properties of the pipe and may consequently affect the analyses for the subsequent tests. Therefore, for the piping system model, the analyses of DM4-2(1) and DM4-2(2) were performed using two approaches: (1) analyses using the initial piping system model and (2) analyses using the deformed piping system model.

Analyses of the elbow model considering the deformed model were not found to produce any plastic strain (for unidentified reasons) and were not presented for comparison. Strain comparisons were based on the average of the strain ratcheting time histories at the four nodes of each element.

DM4-1 Comparisons of the displacement D2 and acceleration A2 are provided in Figure 8. The overall shapes and the peak responses of the time histories agree excellently between the test and the analysis, with a maximum peak difference of about 10% (over-predicted by the analysis). The analytical time histories appear to be slightly less damped than the test. The Fourier spectra of the test displacements show a flat region for frequencies above 20 Hz, indicating white noise in the recorded data that, however, is not noticeable in time history plots due to its relatively small magnitude. The dominant responses, which are at slightly less than 6 Hz, and most responses for frequencies below 10 Hz compare especially well between the test and analysis. At low frequencies, the general trends of the displacement responses are very similar for the test and the analysis, demonstrating similar levels of residual displacements. The response spectra of the acceleration A2 are very close for the test and the analysis. The spectral response peaks are at slightly less than 6 Hz, which is the resonant frequency. The difference between the maximum spectra responses is only about 12% (over-predicted by the analysis), comparing to a difference of about 1% in the ZPA's.

Figure 9 shows the strain comparison between the DM4-1 test and one of the four selected elements. The strain ratcheting phenomena are predicted relatively accurately. Although the first plateau in the analytical hoop strain time history is less than half of that from the test, the hoop strain from the analysis, less the initial elastic strain, is very close to that from the test at the end of the analysis. The axial strain ratcheting is under-predicted. The comparisons for the other three elements were not as good as the one shown in Figure 9; some showed only about 1/6 of the test hoop strain at the end of the analysis. Closer matches in strain comparisons were observed for elements farther away from the strain gauges. This was suspected as being mainly due to the difficulty for the analytical model to represent accurately the complex strain ratcheting phenomena, but also could be possibly due to the variation in the pipe thickness in the test.

DM4-2(2) Figure 10 shows the comparisons of the displacement D2 and the acceleration A2, for the case that considered the plasticity accumulation. No significant difference in these responses can be found between the approach that considered the plasticity accumulation and the approach that did not. Further examination of the displacement

outputs at nodes 30 and 34 found that between these two approaches, two major displacement components DX and RZ did not show much difference while the other four displacement components DY, DZ, RX, and RY showed large differences during the first 20~25 seconds and after that became very similar. This observation implies that the approach without considering the plasticity accumulation may be able to capture the overall behavior of the piping system at a later stage of the analysis. The comparisons of the displacement and acceleration responses for this test have a similar level of accuracy to previous cases.

For the analysis of the elbow model, strains at the end of analysis for the four selected elements were 2 to 5 times of those of the test (see Figure 11 for an example). Because this analysis started with an intact elbow, it might have recovered the plasticity development for the previous tests within the first 20~25 seconds. Just for the sake of argument, if a plasticity level of 0.7% (for DM4-2(1), not shown) and the initial elastic strain were taken out from the hoop strain for this analysis, the resultant final hoop strain would be about 0.9% at the strain gauge location, which is just about 10% higher than the test. As shown in Figure 11, the shape of the strain ratcheting history from the test shows a virtually zero ratcheting zone during the first 20 seconds, which suggests that the deformed piping system can accommodate elastically this part of the input motions (due to shakedown). In contrast, the initial plasticity accumulation in the analysis is very fast and the analytical strain history shows a short plateau of about 0.9% between 10~20 Hz, which imitates the initial flat region in the test strain time history. The axial strains were not significant in magnitude. Similar to previous analyses, it was also found that the calculated hoop strain was larger for elements farther away from the strain gauge location.

The US Tests

JNES/NUPEC provided NRC/BNL the results of the five repetitive tests, designated as US2-1, US2-2, US2-3, US2-4, and US2-5. Only the US2-1 test was considered in the analysis for the US2 series of tests. Since the strain gauge in the hoop direction failed prematurely in the test, a comparison of strain ratcheting history will not be presented.

As shown in Figure 12, the comparisons of the displacement and acceleration for this analysis are not as good as those for the DM tests. The analytical time histories appeared to be less damped than the test. In addition, the analytical time histories strongly indicated that the responses were trimmed from the peaks, especially obvious for the acceleration time history. The large residual displacements in the test were not predicted by the analysis. It appeared that the multi-linear kinematic hardening model might have resulted in shakedown prematurely for this level of input motion. However, the analysis under-predicted the response spectrum peak only by about 10% and the ZPA by about 8%. As shown by the Fourier spectra, the dominant responses at about 3.6 Hz and most responses for frequencies between 2~10 Hz agreed well between the test and analysis. In addition, the spectral responses from the test and the analysis agreed fairly well for the dominant frequency range around 3.6 Hz.

CONCLUSIONS

In the NRC/BNL nonlinear analyses for predicting the seismic response of the JNES/NUPEC large-scale piping system tests, two finite element models were created for the DM tests and the US tests. The first was a piping system model which used plastic pipe elements and multi-linear material models to obtain the displacement and acceleration responses for the entire piping system. The second model was an elbow model that used a finite strain shell element and the Chaboche nonlinear material model to obtain the strain response.

The analyses showed that the piping system model can accurately predict the displacement and acceleration responses for low to moderate input motions and less accurately for high input motions. For the DM tests, it was noted that the plasticity accumulation in the piping system model only affected the performance of the piping system model during the early part of the input motions and did not change the overall response for the entire time histories. The displacement and acceleration responses appeared to be restrained for large input motions that may imply that the multi-linear material model resulted in shakedown behavior. The elbow model predicted relatively accurate strain ratcheting histories compared to test data. However, it was noted that the level of accuracy for the analysis to test strain comparisons was not as good as for the piping system displacement and acceleration response.

Although the material models developed in this paper follow the test curves extremely well, large variations in the test comparisons, particularly for strain and strain ratcheting, were still noted. The nonlinear dynamic characteristics of a large piping system are difficult to predict with high accuracy even when state-of-the-art models and finite element codes are used. In regulatory activities related to piping systems in nuclear power plants, reviewers should be aware of such difficulties and uncertainties in any piping system seismic analysis submittals involving elasto-plastic analysis.

ACKNOWLEDGEMENT

This work was performed under the auspices of the U.S. Nuclear Regulatory Commission, Washington, D.C., which is gratefully acknowledged.

REFERENCES

1. DeGrassi, G., Nie, J., and Hofmayer, C. (2007). "Seismic analysis of large-scale piping systems for the JNES/NUPEC ultimate strength piping test program," Draft NUREG/CR, by Brookhaven National Laboratory for the U.S. Nuclear Regulatory Commission.

2. Borsoi, L. and Ricard, A. (1985). "A simple accelerogram correction method to prevent unrealistic displacement shift," *8th SMIRT*, Vol.**K**(a), Paper K2/7, Brussels.

3. DeGrassi, G. and Hofmayer, C. (2005). "Seismic analysis of simplified piping systems for the NUPEC ultimate strength piping test program," *NUREG/CR-6889*, by Brookhaven National Laboratory for the U.S. Nuclear Regulatory Commission.

4. Chaboche, J.L. (1986). "Time independent constitutive theories for cyclic plasticity," *International Journal of Plasticity*, Vol. **2**, pp. 149-188.

5. Bari, S. and Hassan, T. (2000) "Anatomy of Coupled Constitutive Models for Ratcheting Simulations," *International Journal of Plasticity*, Vol. **16**, pp. 381-409.

6. ANSYS (2007). "Release 11.0 documentation for ANSYS," Online Manual, ANSYS, Inc.

TABLE 1 JNES/NUPEC LARGE-SCALE PIPING SYSTEM TEST LOAD CASES

Test Case			Excitation Wave	Excitation Direction	Design Stress Level	Dominant Frequency
Design Method Confirmation Test	Preliminary Test	DM1-1	Sweep	Horizontal	(Elastic)	—
			Sweep	Vertical	(Elastic)	—
		DM1-2	Seismic	Horizontal	(=DM2-1,2)	Off-resonance
			Seismic	Vertical	(=DM2-1,2)	
	Allowable Stress Test	DM2-1	Seismic	H + V	3Sm (=S2 limit)	Off-resonance
		DM2-2	Seismic	H + V	4.5Sm	
	Elasto-Plastic Response Test	DM4-1	Seismic	H + V	6Sm	On-resonance
		DM4-2(1)	Seismic	H + V	10.5Sm	
		DM 4-2(2)	Seismic	H + V	13.5Sm	
Ultimate Strength Test	Preliminary Test	US1	Sweep	Horizontal	(Elastic)	—
			Sweep	Vertical	(Elastic)	—
	Ultimate Strength Test	US2	Seismic	Horizontal	24Sm	On-resonance

TABLE 2 DM AND US TEST FREQUENCIES AND DAMPING RATIOS FROM SEISMIC TESTS

Test Case	Resonant Frequency (Hz)	Damping Ratio (%)	Maximum Design Stress
DM2-1	6.3	2.1	$3S_m$
DM2-2	6.2	2.3	$4.5S_m$
DM4-1	6	2.4	$6S_m$
DM4-2(1)	6	2.9	$10.5S_m$
DM4-2(2)	5.9	3.4	$13.5S_m$
US2	3.6	4.5	$24S_m$

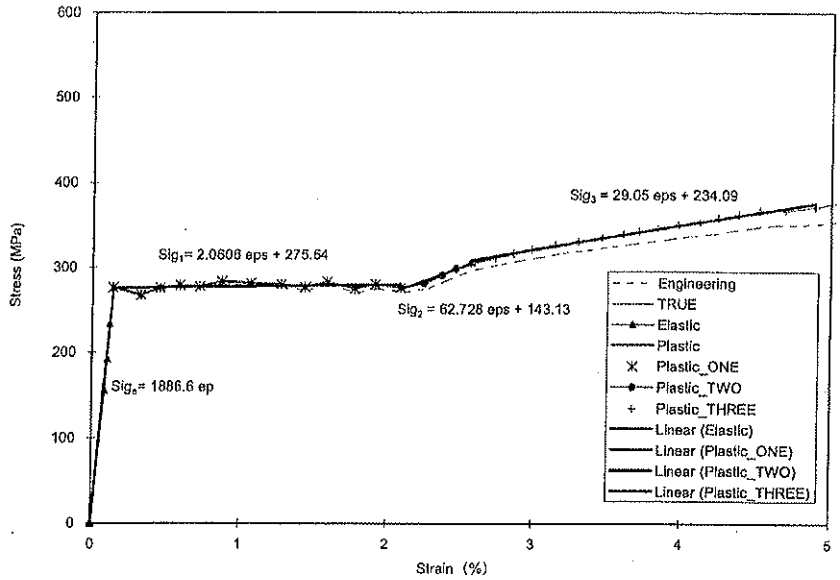

FIGURE 1 MULTI-LINEAR MATERIAL MODEL BY FITTING THE MONOTONIC TENSILE TEST

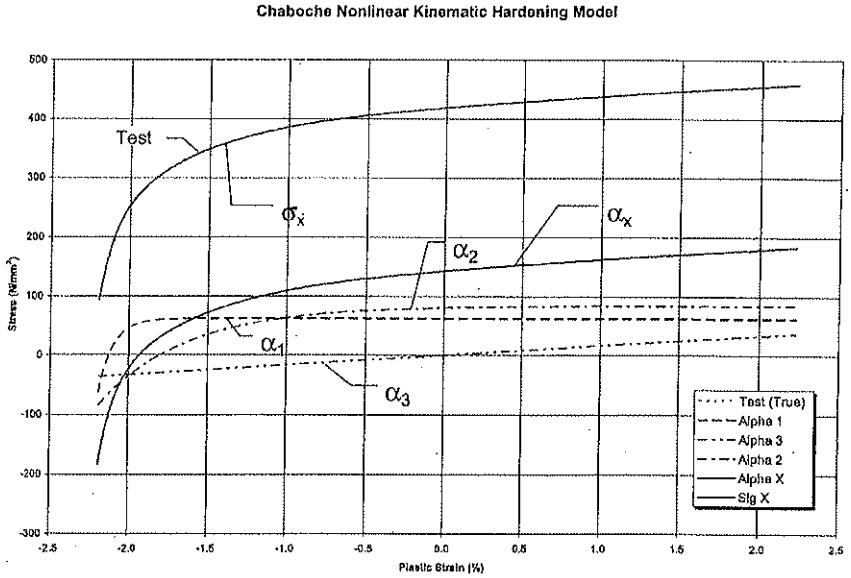

FIGURE 2 CHABOCHE NONLINEAR KINEMATIC HARDENING MODEL (EXCEPT FOR γ_3)

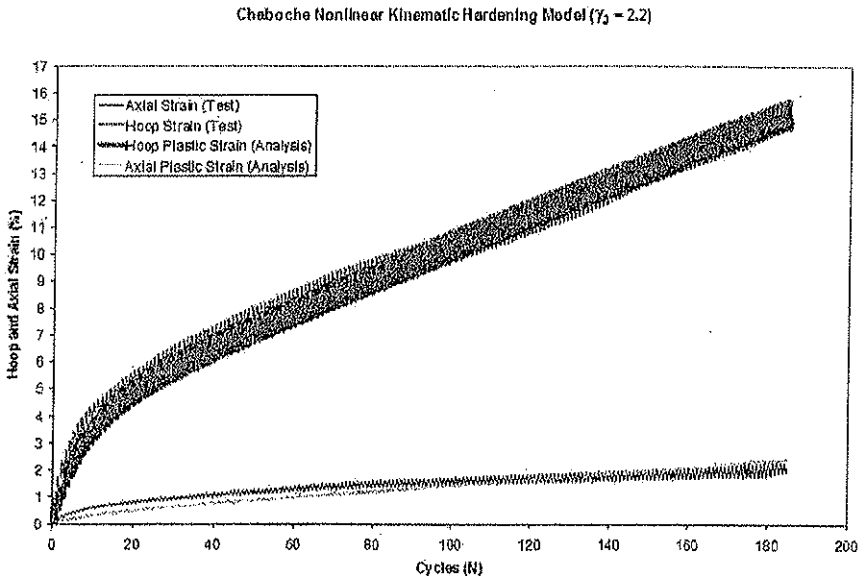

FIGURE 3 HOOP AND AXIAL STRAIN VS. CYCLE AT ELBOW FLANK OF AN ELBOW COMPONENT

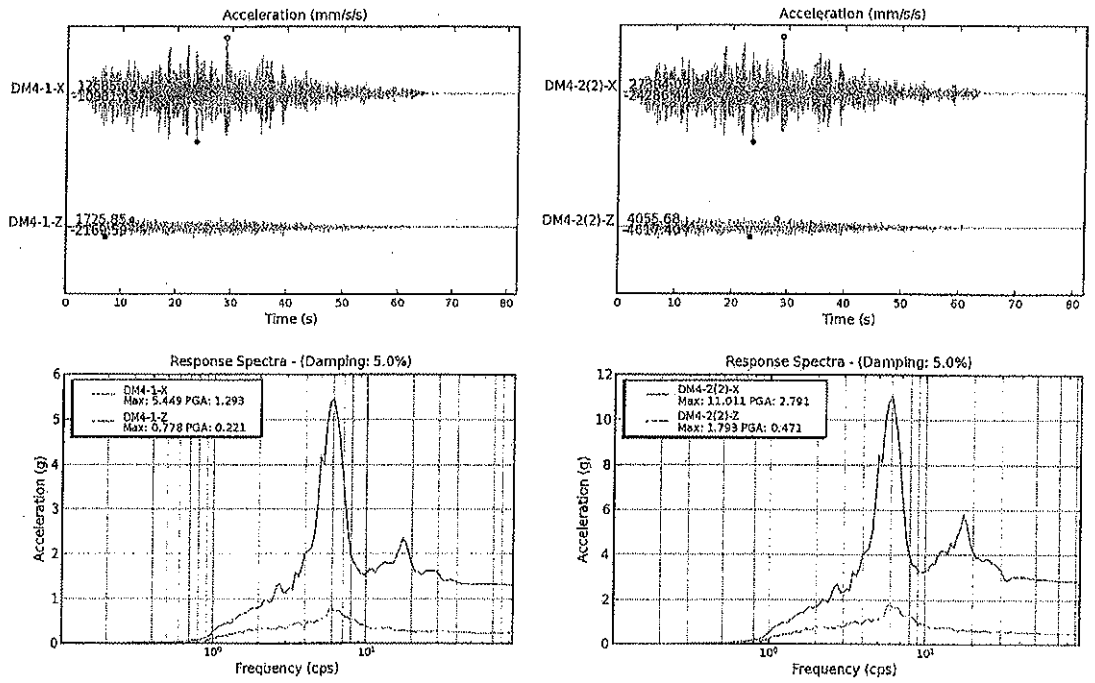

DM4-1 DM4-2(2)

FIGURE 4 HORIZONTAL AND VERTICAL INPUT MOTIONS AND THEIR 5% RESPONSE SPECTRA FOR DM4-1 AND DM4-2(2)

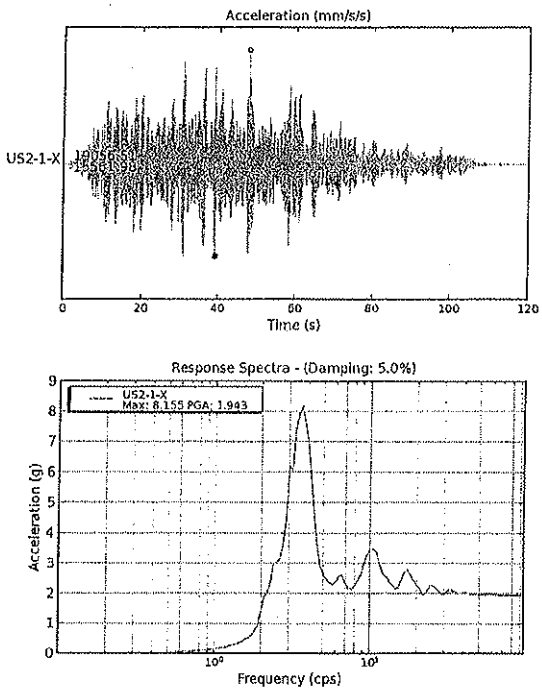

FIGURE 5 HORIZONTAL INPUT MOTION AND ITS 5% RESPONSE SPECTRA FOR US2-1

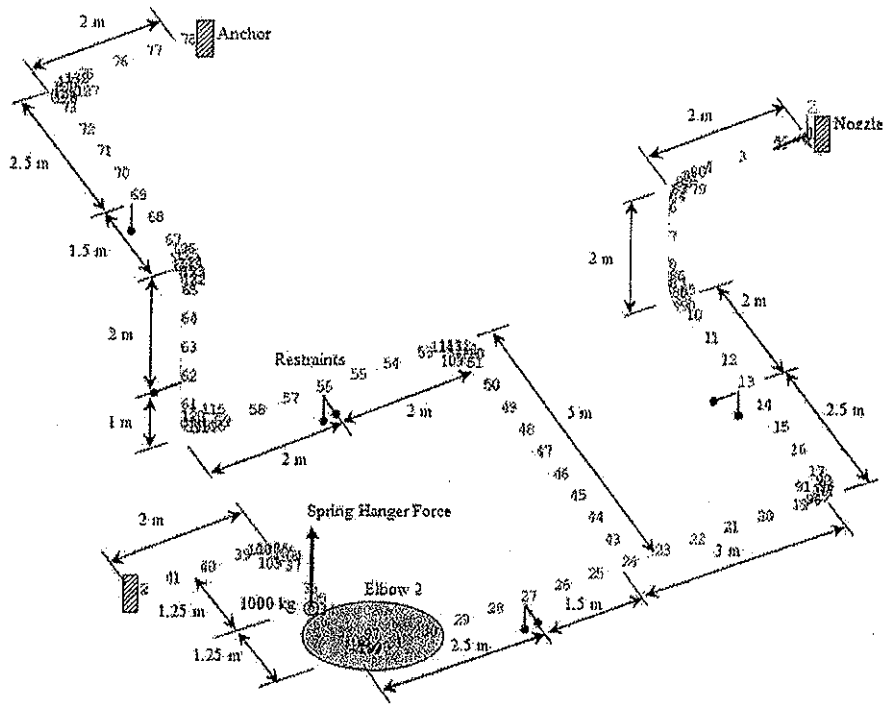

FIGURE 6 PIPING SYSTEM FE MODEL USING PIPE ELEMENTS FOR DM TESTS

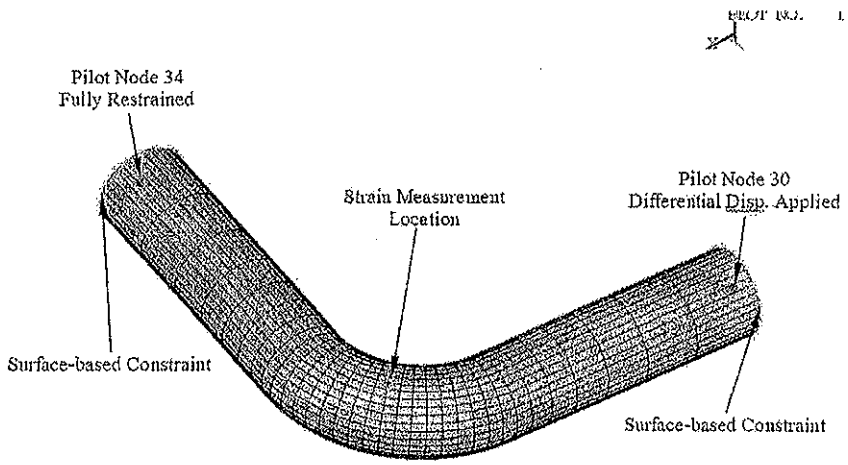

FIGURE 7 ELBOW 2 SHELL MODEL FOR DM AND US TESTS

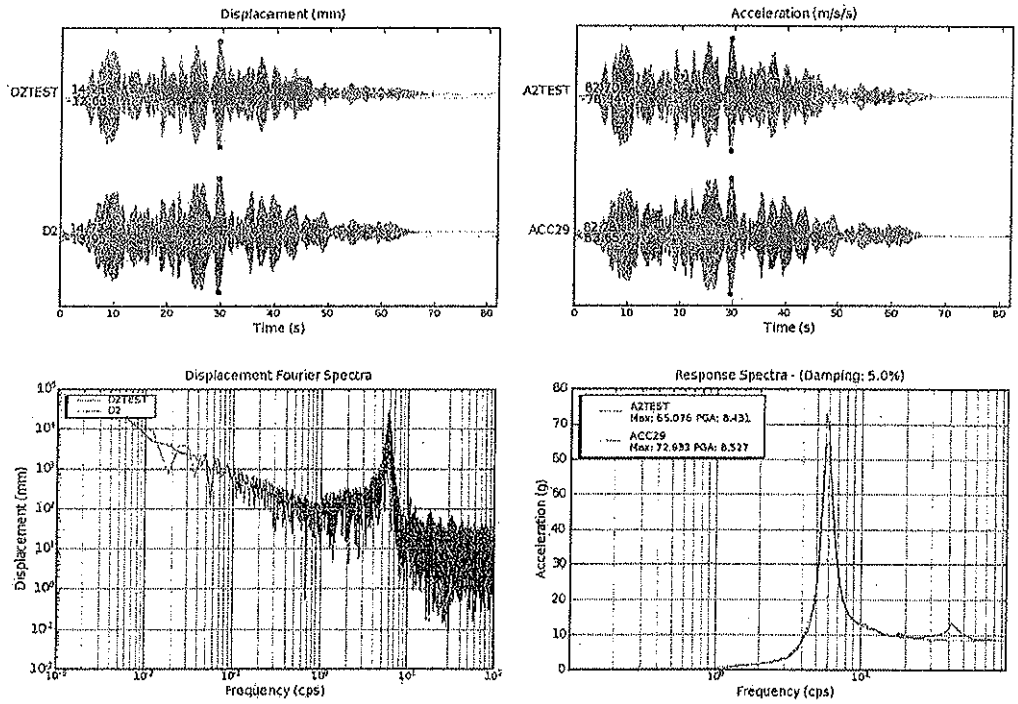

FIGURE 8 COMPARISONS OF DISPLACEMENT D2 & ACCELERATION A2 FOR DM4-1

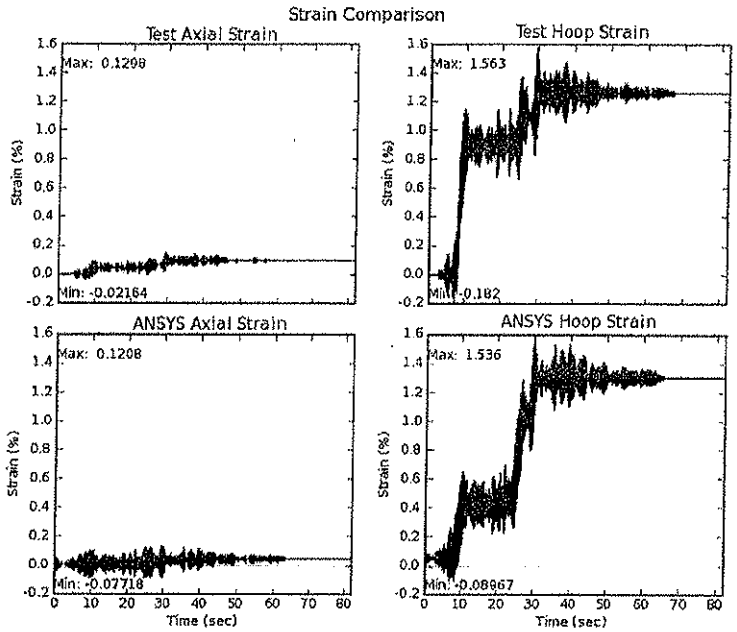

FIGURE 9 STRAIN RATCHETING COMPARISON AT ELEMENT 145 FOR DM4-1

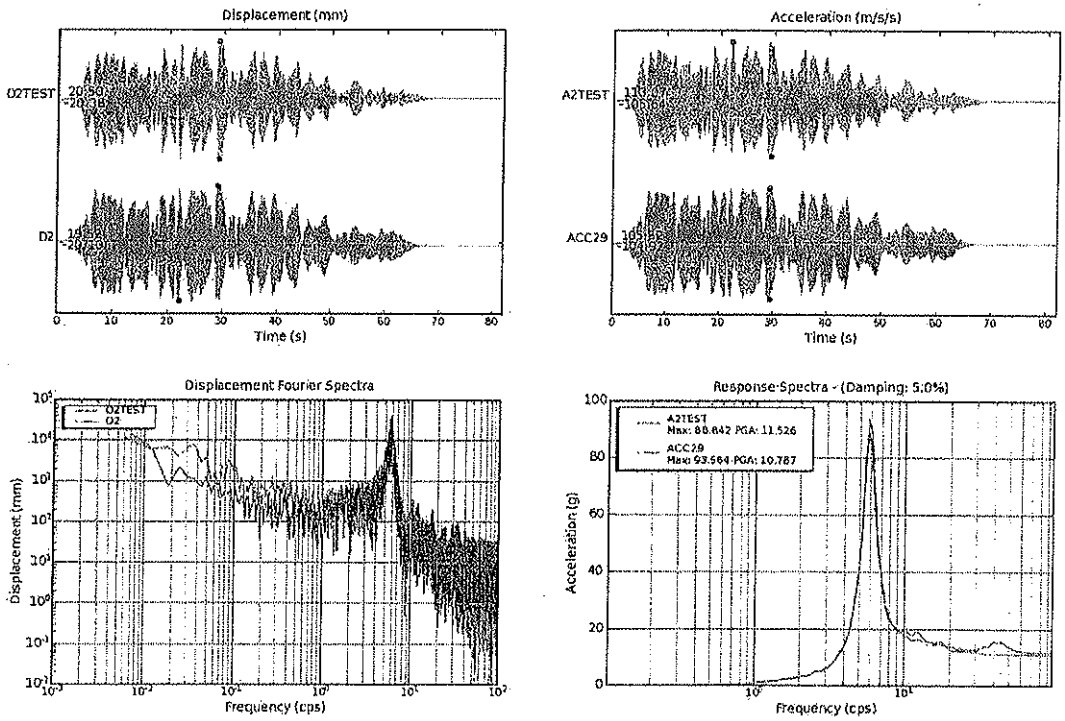

FIGURE 10 COMPARISONS OF DISPLACEMENT D2 & ACCELERATION A2 FOR DM4-2(2) (DEFORMED PIPE)

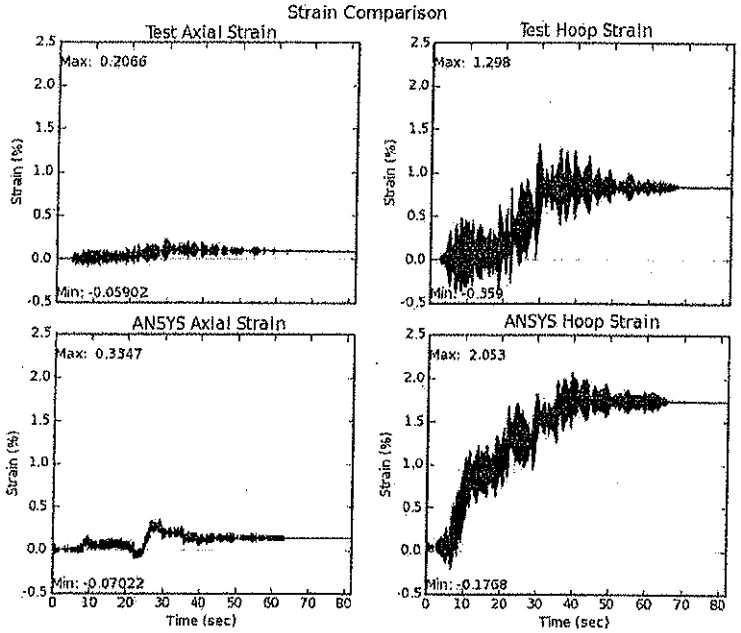

FIGURE 11 STRAIN RATCHETING COMPARISON AT ELEMENT 154 FOR DM4-2(2) (INTACT PIPE)

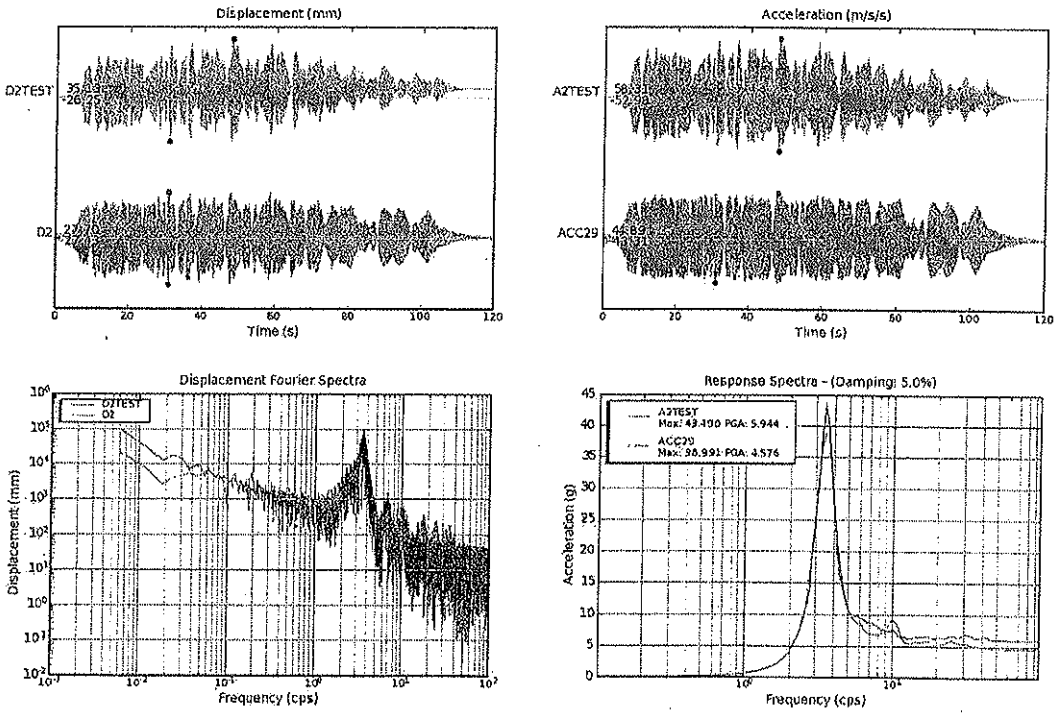

FIGURE 12 COMPARISON OF DISPLACEMENT D2 & ACCELERATION A2 FOR US2